1-1-2005

Characterisation and bending modeling of conducting polymer actuators for use in micro/nano manipulation

G. Alici
University of Wollongong, gursel@uow.edu.au

B. Mui
University of British Columbia, Canada

C. Cook
University of Wollongong, chris_cook@uow.edu.au

2005 IEEE International Conference on Robotics and Biomimetics

Characterisation and Bending Modeling of Conducting Polymer Actuators for Use in Micro/Nano Manipulation

Gürsel ALICI
School of Mechanical, Materials and Mechatronics Engineering
University of Wollongong
2522, NSW, Australia

Brian MUI
Department of Electrical and Computer Engineering
University of British Columbia
Vancouver, BC, Canada

Chris COOK
Faculty of engineering
University of Wollongong
2522, NSW, Australia

***Abstract* -- As research efforts towards making functional micro/nano robotics systems gather more momentum, there is an increasing need for new actuators that can not only be suitable to miniaturization, but also be free from sliding and rolling elements so that they can generate a motion resolution and accuracy in a submicron range. Conducting polymer actuators have many promising features to satisfy such a strict requirement. Before introducing them to the micro/nano robotics world, it is necessary to investigate into their actuation mechanism and the smallest displacement they can generate. In this paper, we report on the characterization and modelling of a strip-type fourth generation polyprrole polymer (PPy) actuator, which operate in a non-liquid medium, i.e. in the air. After deriving a mathematical model approximately accounting for mechanical, electrical, and chemical properties and geometric parameters of the actuator, the model has been experimentally verified for an actuator with the dimensions of (10mm x 1mm x 0.21mm). Theoretical and experimental results are presented to demonstrate that the model is effective enough to predict the displacement output of the strip type-PPy actuator all along the edge of the actuator as a function of the applied voltage.**

***Index Terms* – conducting polymer actuators, micro/nano manipulation, mathematical modeling**

I. INTRODUCTION

Polymers derived from pyrrole, aniline or thiophene can be used as Conducting Polymer (CP) actuators or artificial muscles [1], [2]. The CP actuators based on pyrrole is known as polypyrrole (PPy) actuator. When the polymer is doped electrochemically, ions are sent inside the polymer causing volume expansion. Applying voltages as small as 1 V controls the volume change of the polymer in the form of expansion and contraction. The change in the volume generates a bending displacement. This follows that the electrochemical energy is converted into mechanical energy. There has been significant amount of research on conducting polymer actuators and their use in various applications in the last decade [1-5]. A comprehensive account of polymer actuators is given in [3 ,6].

Conducting polymer actuators have attracted the attention of some researchers as potential actuators and sensors for micromanipulators [3,5,7,8]. For example, Zhou et al. [3] have reported on three types of polymer actuators including ionic conducting polymer film actuators, polyaniline actuators, and parylene thermal actuators. They have presented their fabrication and performance results. Smela et al. [5] have presented the development and performance outcomes of PPy and Au bilayer conducting polymer actuators operating in electrolyte solutions. As an extension of this study, Jager et al. [7] have fabricated a serially connected micromanipulator to pick, move, and place 100μm glass beads. It has been demonstrated that the micromanipulator is very suitable for single-cell manipulation. Liu et al. [8] have presented a fabrication technique to make a microstructure consisting of a polymer substrate Kapton and PPy/Au bilayer. Madden et al. [9] conducted stress-strain tests under constant applied potential to determine the stiffness of PPy actuators. Further, relationships between strain and charge, and stress and strain are developed and then combined with the stiffness model to describe the electromechanical response of the PPy actuator. Nemat-Nasser and Li [10,11] have established a micromechanical bending motion model to characterize 'electrochemomechanical' response of an ionic polymer-metal composite actuator consisting of Nafion and platinum bilayer. The model is based on the micromechanics theory [11] that electrically unbalanced negative ions permanently fixed to the Nafion polymer generate the internal stresses. The parameters in the model are estimated using experimentally measured tip displacement. To the best of our knowledge, this is the only model in the literature accounting for the electrical, chemical, and mechanical properties of an ionic polymer actuator. A similar modeling approach should be pursued for conducting polymer actuators. We claim that the model developed in this study is a significant contribution towards a physics-based mathematical model to understand and predict the complex behavior of PPy actuators. Please note that the model developed in this study can predict the horizontal and vertical displacements of the PPy actuator all along its edge.

This study is a part of an ongoing-project on the establishment of micro/nano manipulation systems such as grippers and planar mechanisms articulated with the fourth generation PPy actuators, which are fabricated at the Intelligent Polymer Research Institute at the University of Wollongong [1]. Conducting polymers have many promising features including low actuation voltage, operation in aquatic mediums and in air, low cost, high force output to weight ratio, and are very suitable to open-loop control. Their main drawback is their low

0-7803-9315-5/05/$20.00 ©2005 IEEE

speed of response and nonlinearity due to their actuation principle, which is based on mass transfer. The application of conducting polymer actuators is an emerging field as researchers begin to harness the benefits of their material properties, which are greatly enhanced at smaller scales [6]. Possible future applications include artificial muscles, and a wide variety of sensors and actuators in biomedical systems [2] and micro/nano manipulation systems. As these actuators do not contain any rolling and sliding elements, they are especially suitable to micro/nano manipulation tasks.

Because the actuation mechanism is largely based on material properties, characterization of these properties with respect to actuation and establishment of a mathematical model predicting the bending motion have been the main focus of current work. However, there are a large number of variables and interrelated parameters that affect the actuation. The complex nature of the actuation mechanisms and lack of analogous classical theories have hindered the development and conclusive experimental verification of comprehensive models of the actuator behaviors. In this study, we establish a physics-based mathematical model to predict the bending motion of PPy conducting polymer actuators, to be dedicated to micro/nano manipulation mechanisms, which are currently under fabrication in our laboratory. After deriving the mathematical model, the model has been experimentally verified for an actuator with the dimensions of (10mm x 1mm x 0.21mm). The model predicts the bending motion/curve of the actuators as a function of the applied voltage quite well.

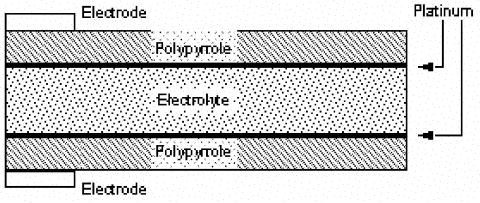

Figure 1: Layered structure of PPy actuator.

II. ACTUATOR STRUCTURE

The conducting polymer actuator considered in this study consists of a five-layer structure, with the polypyrrole (PPy) as the electroactive component [1]. The layered structure is shown in Figure 1. The outside layers of polypyrrole are clamped to each layer with two electrodes at one end of the actuator strip. Thin layers of platinum are sputter-coated to a thickness of about 10 to 100 angstroms, and serve to increase the conductivity between the electrolyte and PPy layers. The electrolyte layer in the middle is polyvinylidine fluoride (PVDF), with a thickness of 110μm. The PVDF is an inert, non-conductive, porous polymer that serves as the electrochemical cell separator. It also serves as a reservoir for the electrolytic ions tetrabutylammonium hexafluorophosphate ($TBA{\cdot}PF_6$) in an organic solvent propylene carbonate (PC) at a concentration of 0.25M. Strips of varying lengths and widths are easily produced after synthesis of the film.

A. Actuation Mechanism and Properties

Deflection in the actuator strip is achieved by applying an electric potential across the electrodes. A redox reaction occurs as a result of this applied potential, as electrons conduct from one polypyrrole layer to the other. The PF_6^- anions then move through the electrolyte into the oxidized PPy layer, and move out of the reduced PPy layer to neutralize the charge imbalance created by the movement of electrons. The chemical process is expressed below:

$$PPy^+(PF_6^-) + TBA^+ + e^- \leftrightarrow PPy^\circ(TBA{\cdot}\,PF_6^-)$$
(*doped, oxidized state*) (*undoped, reduced state*)

The displacement of PF_6^- ions causes material strain in the PPy layers through a number of effects. One is the effect of the gain or loss of ion volume causing volume expansion or contraction in the PPy layers. The movement of solvent molecules, which accompany the ion diffusion, also contributes to volume change in the PPy layers. The other factor is the resultant electrostatic forces between the displaced ions and the polymer backbone that cause the PPy layers to expand or contract. As the two PPy layers undergo opposing strains, a bending moment is induced, causing deflection of the actuator.

B. Electrical Properties

Because the actuator is driven by electrical input, it is important to characterize the electrical properties of the actuator. As previously discussed, an applied potential is used to control the oxidation state, or doping level of the conducting polymer. The effect of this potential can be characterized through impedance and current. The impedance of conducting polymers is capacitive at lower frequencies, and is nearly resistive at high frequencies [9, 12]. Correspondingly, it has also been demonstrated that current approaches zero as the polymer layer becomes completely oxidized or reduced, though it should be noted that small currents are required to maintain full reduction [5]. Nevertheless, the impedance, and consequently the current, both vary with the oxidation state, or applied potential. The relationship between current and voltage has been shown to exhibit hysteresis behavior [13].

C. Chemical Properties

The chemical properties of conducting polymers have a significant effect on the actuation mechanism. In addition to impedance and capacitive charging effects described in the previous subsection, the rate of diffusion is another significant parameter that limits the response time of the actuator. The parameters that contribute to this property include the dopant molecule size, the polymer matrix structure, the electrolyte concentration, and the electric potential gradient [14]. While the deflection in conducting polymer actuators has been attributed in part to the electrostatic forces between displaced ions and the polymer backbone [10,13], it has been suggested that the dominant actuation mechanism is due to the voluminous displacement of ion and solvent molecules [5,9,15]. The amount of deflection of the actuator has also been shown by Kaneko et al [13], to depend on the molecular properties of the dopant. Ions with larger molecular weights produce larger strain than ions with smaller molecular weights.

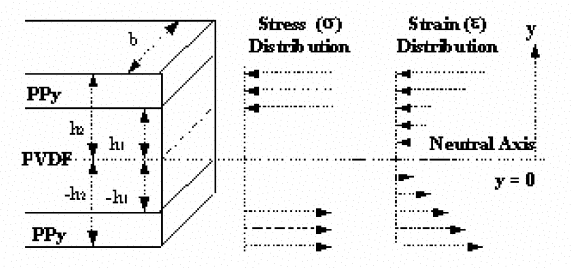

Figure 2: Stress and strain distribution model for a cross section.

D. Mechanical Properties

The primary mechanical properties relating to the actuation mechanism include strain, elastic modulus, and the physical dimensions of each layer. Opposing strains in the two polymer layers result in deflection of the actuator. The volume change in the polymer is closely related to the amount of charge and solvent that is transferred from layer to layer, and it has been shown that the material strain is linearly related to current density (mA/cm^2) and exchanged charge density (C/mm^3) up to the point of material degradation [1,9,16]. In light of this fact, the strain-voltage relationship exhibits the same hysteresis behavior as the current-voltage relationship [5]. The presence of a strain gradient along the thickness of the actuator has been observed at times shorter than the diffusion time constant [12]. The elastic modulus of conducting polymer actuators has been shown to depend on a number of factors. The elastic modulus is constant for a limited range of magnitude of applied potentials, but increases when the potential is beyond this range [16]. It has also been suggested that the elastic modulus varies with frequency [12]. Various research groups have also investigated the effect of layer thicknesses. Because the actuation depends on the redox reaction, the polymer layer would require a fixed amount of charge to fully oxidize or reduce depending on the layer thickness [5].

III. ACTUATOR MODELING

The goal is to develop a simple, practical means of describing the bending motion of conducting polymer actuators in terms of the input voltage, geometric parameters, and material properties.

A. Modeling Assumptions

(i) The material properties of the platinum layers are neglected, due to their small thickness (10-100 Angstroms) relative to the PPy and PVDF layers.

(ii) The internal stresses in the actuator are caused solely by the expansion or contraction of the two PPy layers, as seen in Figure 2. This assumption enables the differentiation between the 'active' components of the actuator (PPy) and the 'passive' components (PVDF). These stresses are assumed to be in the lateral direction only, uniform within each PPy layer, with opposite signs relative to the opposing PPy layer. Uniform stress distributions in the PPy layers also imply that the PPy thickness is within a certain limit of thickness, for this assumption to hold true. For PPy thicknesses beyond this limit, the redox reaction occurring in the PPy is less effective in the portions of PPy further from the PVDF layer.

(iii) As depicted in Figure 2, the resulting strain distribution varies linearly along the thickness of the actuator strip with respect to the distance from the neutral axis. This is a fundamental assumption in bending analysis of materials and structures, whereby plane cross-sections remain plane upon bending.

Using these three key assumptions, the bending curve model is derived for an internal bending moment due to the expansion or contraction of PPy, which causes the deflection of plane cross-sections in the actuator strip.

B. Exchanged Charge

As previously discussed in Section 2, the mechanical behavior of conducting polymer actuators is known to be linear with exchanged charge. Because the methods of this study utilize an applied voltage as the control input, a relationship must be established to relate this applied voltage to the exchanged charge between the PPy layers. This will eliminate the need to consider the unpredictable hysteresis effects in the analysis. To accomplish this, we utilize the classical relation for a steady-state response between voltage and charge via capacitance as defined by

$$\Delta Q = \Delta V . C \tag{1}$$

where the exchanged charge, ΔQ, is directly related to the applied voltage, ΔV, and the capacitance, C. The current response of the actuator considered in this study is recorded as shown in Figure 3.

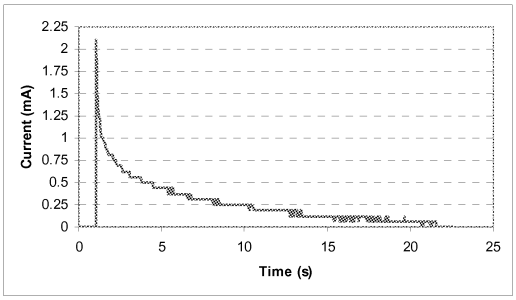

Figure 3: Experimental current response of the actuator under a voltage step input.

From this data, the capacitance can be calculated by multiplying each current data point by its time increment of 0.05 second, and dividing by the magnitude of the step voltage input. It is expected that because the time required for the current to reach zero is on the order of tens of seconds, the small time increment is a sufficient approximation to full integration of the current data.

C. Internal Bending Moment

Based on the stress distribution depicted in Figure 2, an expression for the driving force of the actuator, the internal bending moment M, can be derived by integrating the uniform stress σ, acting over the cross-sectional area of the PPy layers,

in terms of the distance from the neutral axis y, and the actuator width b, [17].

$$M = \underbrace{\int \sigma\, y\, dA}_{Bottom\ PPy} + \underbrace{\int -\sigma\, y\, dA}_{Top\ PPy} \Rightarrow M = \sigma b \int_{h_1}^{h_2} y\, dy - \sigma b \int_{-h_2}^{-h_1} y\, dy \quad (2)$$

$$M = b\sigma\left(h_2^2 - h_1^2\right)$$

As previously discussed in Section II.D, it has been experimentally determined that the strain in conducting polymers is linearly proportional to the exchanged charge density or current density [1,16]. While this relationship is often documented in terms of strain, a more accurate expression for this relationship is that the stress varies linearly with exchanged charge density. This is because the exchanged charge density is directly responsible for causing internal stress in the material independently of any other factors, including external forces that may restrict strain and bending. Thus, the stress can be expressed as

$$\sigma = \alpha \frac{\Delta Q}{B} \quad (3)$$

where the stress σ, the exchanged charge ΔQ, and the volume of a PPy layer in the actuator B are related to each other via a coefficient α. The direction of σ is determined by whether ΔQ is positive or negative. Substituting Eq.3 into Eq.2 gives

$$M = b\alpha \frac{\Delta Q}{B}\left(h_2^{\,2} - h_1^{\,2}\right) \quad (4)$$

Using current control, this expression is sufficient for experimental validation. However, to avoid damaging the actuators with excessively high potentials that may occur when using current control, voltage control is used instead. Thus, for cases in which a steady state step voltage is used as the control input, we can substitute the voltage, capacitance, charge relation $\Delta Q = \Delta V \cdot C$ as described in Section III to obtain

$$M = \alpha b \frac{\Delta V C}{B}\left(h_2^{\,2} - h_1^{\,2}\right) \quad (5)$$

Finally, the volume of a PPy layer B, is expressed in terms of the actuator width b, length L, and the boundaries of the PPy layer shown in Figure 2.

$$B = bL\left(h_2 - h_1\right) \quad (6)$$

Thus, the internal bending moment resulting from the stresses in the PPy layers can be expressed as

$$M = \frac{\alpha \cdot b \cdot \Delta V \cdot C\left(h_2^{\,2} - h_1^{\,2}\right)}{bL\left(h_2 - h_1\right)} \Rightarrow M = \frac{\alpha \cdot \Delta V \cdot C\left(h_1 + h_2\right)}{L} \quad (7)$$

D. Bending Curve Model

As previously discussed, assuming the strain distribution is as depicted in Figure 2, then an equivalent expression for the internal bending moment can be derived whereby the stress distribution matches the linear strain distribution. By geometry, with reference to Figure 4, for an incremental length of the actuator strip, dx, an incremental bending angle, $d\theta$, and a distance from the neutral axis y, we can express the strain, ε, as

$$\varepsilon = y \cdot \frac{d\theta}{dx} \quad (8)$$

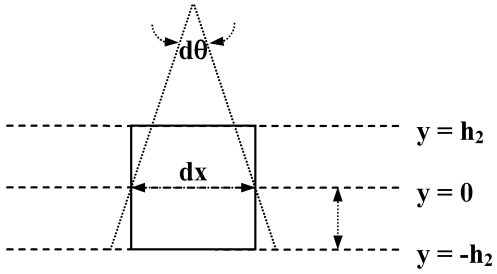

Figure 4: Expansion in actuator for incremental length dx.

From Hooke's Law, we obtain

$$\frac{\sigma}{E} = \varepsilon = y \cdot \frac{d\theta}{dx} \quad (9)$$

Thus, for the PPy layers and the PVDF layers, the respective stresses are

$$\sigma_{PPy} = E_{PPy} y \cdot \frac{d\theta}{dx} \quad (10)$$

$$\sigma_{PVDF} = E_{PVDF} y \cdot \frac{d\theta}{dx} \quad (11)$$

The area moments of inertia depends on the width of the strip, and the thickness of the layers with reference to the geometric dimensions shown in Figure 2, and can be expressed as

$$I_{PPy} = \frac{2b\left(h_2^{\,3} - h_1^{\,3}\right)}{3} \quad (12)$$

$$I_{PVDF} = \frac{2bh_1^{\,3}}{3} \quad (13)$$

The internal bending moment can then be expressed in terms of these stresses and area moments of inertia by

$$M = \int_{A_{PVDF}} \sigma_{PVDF} \cdot y dA + \int_{A_{PPy1}} \sigma_{PPy} \cdot y dA + \int_{A_{PPy2}} -\sigma_{PPy} \cdot y dA \quad \Rightarrow$$

$$M = E_{PVDF} \frac{d\theta}{dx} b \int_{h_1}^{h_1} y^2 dy + E_{PPy} \frac{d\theta}{dx} b \int_{h_1}^{h_2} y^2 dy - E_{PPy} \frac{d\theta}{dx} b \int_{h_2}^{h_1} y^2 dy$$

$$M = \frac{d\theta}{dx}\left[E_{PVDF} \underbrace{\left(\frac{2b\left(h_1^{\,3}\right)}{3}\right)}_{I_{PVDF}} + E_{PPy} \underbrace{\left(\frac{2b\left(h_2^{\,3} - h_1^{\,3}\right)}{3}\right)}_{I_{PPy}} \right] \quad (14)$$

The elastic moduli are considered constants because the applied potentials under consideration for this study are within the range for which this is true, as discussed in Section II. The term $d\theta/dx$ represents the amount of bending that occurs at an

incremental length of actuator strip. To obtain a bending curve corresponding with this term, an expression can be derived in terms of the vertical deflection of an actuator strip *v*, and the horizontal distance along the strip in its neutral, straight position, *x*, as shown in Figure 5.

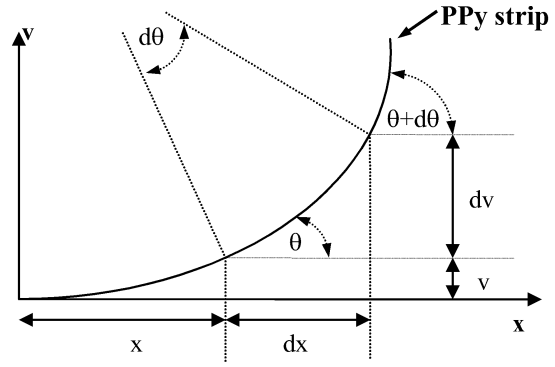

Figure 5: Bending curve of a PPy strip.

For each incremental length of an actuator strip, the vertical displacement *dv*, horizontal position *dx*, and angle of rotation θ, are related by:

$$\theta = arctan\left(\frac{dv}{dx}\right) \tag{15}$$

The incremental angle of rotation differentiated with respect to the *x* direction, gives

$$\frac{d\theta}{dx} = \frac{d}{dx}\left[arctan\left(\frac{dv}{dx}\right)\right] = \frac{\frac{d^2v}{dx^2}}{1+\left(\frac{dv}{dx}\right)^2} \tag{16}$$

Substituting Eq.16 into Eq.14 describing the internal bending moment produces the following nonlinear second-order differential equation;

$$v'' - \left[1+(v')^2\right]\frac{M}{E_{PPy}I_{PPy} + E_{PVDF}I_{PVDF}} = 0 \tag{17}$$

Substituting Eqs. 7,12 and 13 into Eq.17, we obtain the fully expanded equation

$$v'' - \left[1+(v')^2\right]\frac{3\alpha VC(h_2+h_1)}{2bL\left[E_{PPy}\left(h_2^{\,3}-h_1^{\,3}\right)+E_{PVDF}h_1^{\,3}\right]} = 0 \tag{18}$$

IV. MODEL VALIDATION

The actuator strips used in experimentation have the layered structure described in Section 2. To gauge the deflection of actuator strip, the grid paper is placed behind the actuator strip, as shown in Figure 6. The platinum wires on the electrode clamps are connected to the outputs of a potentiostat/galvanostat, controlled using Chart 4 Windows software via a Powerlab 4/20 controller. This software also logs electrical data. Experimental bending curves are obtained by capturing images of the actuator strip at steady state, similar to the image shown in Figure 6. Different voltage step inputs were applied across the strip, with neutralization process performed between each step to eliminate hysteresis effects. Steps were held long enough to allow the current to reach zero, and the bending or force output to reach a steady state.

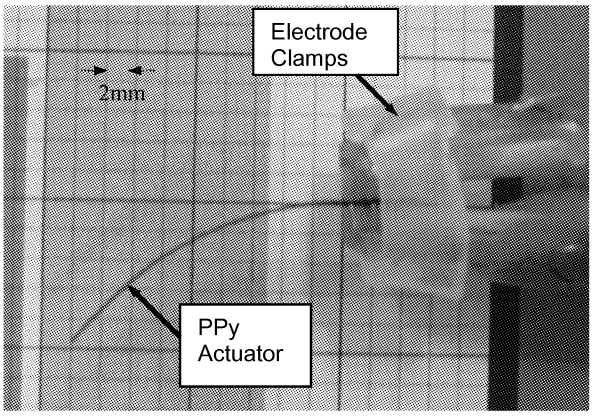

Figure 6: Experimental setup.

Equation 18 has been solved numerically. The voltage *V*, layer dimensions, *L*, *h*, and *b*, are all predetermined constants. The elastic moduli are taken to be 80MPa for E_{PPy} and 440MPa for E_{PVDF} [13]. The capacitance *C*, is calculated from the electrical data, with the current multiplied by each time increment and dividing by the applied potential. The vertical position, *v*, is solved with respect to horizontal position *x* to obtain a theoretical bending curve. Best-fit values of α are found by comparing theoretical bending curves with experimental data for a single actuator at different applied potentials. A constant α is then chosen and used to simulate the bending curves the actuator strip at the same voltage inputs, to verify the model.

While it was expected that α would be constant for a given actuator strip, it was found that for initial tests, the best-fit values of α were actually quite wide-ranging. However, further tests with the same actuator strip showed that the variations in values of α decreased, eventually settling to fairly consistent value. This effect is in agreement with the findings of Spinks et al. [1], whereby it was demonstrated that there was considerable decay in the strain response within the first cycles of testing. After some number of cycles, the strain response showed much more consistency. Taking this into account, each actuator strip tested was cycled for at least 20 cycles prior to recording data.

A. Results and Discussion

The experimental procedure described in the previous section was performed on the actuator strip with the length of 10mm, the width of 1mm, PVDF thickness of 0.110mm, and the PPy layer thicknesses of 0.050mm each, voltage step inputs of 0.2V, 0.4V, 0.8V, and 1.0V were applied. The comparison of experimental bending curves with the theoretical bending curves generated with a constant α value of $0.145(F/m^2)/(C/m^3)$, is shown in Figure 7. These curves follow

the experimental curves quite closely. It should be noted that the model does not account for bending beyond 90 degrees, which is why the tips of the curves with larger deflections show the greatest discrepancy, while the rest of the strip shows better agreement. The results also indicate that the model is valid to predict the horizontal and vertical displacements of the PPy actuator all along its edge.

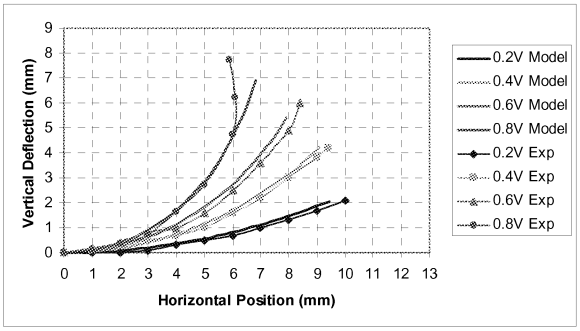

Figure 7: Experimental and theoretical bending curves (10mm x 1mm x 0.21mm, $\alpha = 0.145$).

These results indicate that α can be considered a constant for a given actuator strip. This is significant, considering that this coefficient is a rather complex parameter. It essentially encapsulates much of the actuation mechanism described in Section II whereby exchanged charge causes the migration of dopant ions and solvent molecules, which in turn causes the volume changes in the PPy layers via voluminous displacement and electrostatic forces. The coefficient α quantifies the expansion or compression force density resulting from these effects, per unit of exchanged charge density.

As PPy actuators do not contain any rolling and sliding components, we propose to use them as flexure joints in a number of micro/nano manipulation systems under fabrication in our laboratory. The active PPy strips in a mechanism will act as actuators and joints, which is what we call the *active flexure (act-flex)* joint.

V. CONCLUSIONS

An analysis of the static characteristics of conducting polymer actuator strips has been presented, resulting in the development of a mathematical model of the bending curves produced in response to step input applied potentials. It has been demonstrated that the bending curve model is valid to predict the bent configuration of the actuator for various applied potentials. Tuning the model to fit the bending curve for a given applied potential enables accurate prediction of bending curves for the same actuator under different applied potentials. The model can then be used to predict the effects of parameter variation on various output characteristics. Future work involves (i) investigating into the minimum displacement they can generate in order to make micro/nano manipulation mechanisms articulated by PPy actuators, (ii) analysis, characterization and performance of such mechanisms including the static and dynamic characteristics of the PPy actuators and joints.

ACKNOWLEDGEMENTS

This project has been partly funded by a URC Small Grant. The authors would like to thank a number of people from the Intelligent Polymer Research Institute for providing the actuators, allowing us to use their research facilities, more importantly sharing their sterling expertise with us. These people are Prof. Dr. G.M. Spinks, Prof. Dr. G. G. Wallace, and Mr. Yanzhe (Richard) Wu. Useful discussions with the visiting student, Mr. Philippe Metz, from Institut Francais De Mecanique Avancee (IFMA) are also greatly appreciated.

REFERENCES

1. G. M. Spinks, B. Xi, D. Zhou, V. T. Truong, and G. G. Wallace, "Enhanced control and stability of polypyrrole electromechanical actuators", Synthetic Metals, Vol.140, pp. 273 – 280, 2004.
2. E. Smela, "Conjugated Polymer Actuators for Biomedical Applications", Advanced Materials, Vol.15, No.6, pp. 481 – 494, March 2003.
3. J. W. L. Zhou, H. Y. Chan, T. K. H. To, K. W. C. Lai, and W. L. Li, "Polymer MEMS actuators for underwater micromanipulation", IEEE/ASME Trans. on Mechatronics, Vol.9, No.2, pp. 334 – 342, 2004.
4. E. W. H. Jager, E. Smela, O. Inganas, and I. Lundstrom, "Polypyrrole Microactuators", Synthetic Metals, pp. 1309 – 1310, 1999.
5. E. Smela, M. Kallenbach, and Jens Holdenried, "Electrochemically Driven polypyrrole bilayers for moving and positioning bulk micromachined silicon plates", IEEE Journal of Microelectromechanical Systems, Vol.8, No.4, pp. 373 – 383, December 1999.
6. R. H. Baughman, "Conducting polymer artificial muscles," Synthetic Metals, vol. 78, pp. 339-353, 1996.
7. E. W. H. Jager, O. Inganas, and I. Lunstrom, "Microrobots for Micrometer-size objects in Aqueous Media: Potential tools for Single Cell Manipulation", Science, Vol.288, pp 2335 – 2338, June 30, 2000.
8. Y. Liu, L. Oh, S. Fanning, B. Shapiro, and E. Smela, "Fabrication of Folding Microstructures Actuated by Polypyrole/Gold Bilayer", IEEE 12th International Conference on Solid state Sensors, Actuators and Microsystems, Boston, pp. 786 – 789, June 2003.
9. J. D.W. Madden, P. G.A. Madden, I. W. Hunter, "Polypyrrole actuators: Modeling and performance," in Proc. SPIE Smart Structures and Materials: Electroactive Polymer Actuators and Devices, vol. 4329, 2001, pp. 72-83.
10. S. Nemat-Nasser, J.Y. Li, "Electromechnanical response of ionic polymer-metal composites," J. Applied Physics, vol. 87, no. 7, pp. 3321-3331, 2000.
11. S. Nemat-Nasser, "Micro-mechanics of Actuation of Ionic Polymer-metal Composites," J. Applied Physics, vol. 92, no. 5, pp. 2899-2915, 2002.
12. M. Shahinpoor, K.J. Kim, "Ionic polymer-metal composites – fundamentals and phenomenological modeling," in Proc. SPIE Smart Structures and Materials: Electroactive Polymer Actuators and Devices, vol. 4695, 2002, pp. 294-302.
13. M. Kaneko, M. Fukui, W. Takashima, K. Kaneto, "Electrolyte and strain dependencies of chemomechanical deformation of polyaniline film," Synthetic Metals, vol. 84, pp. 795-796, 1997.
14. T. F. Otero, H. Grande, J. Rodriguez, "An electrochemical model for the electrochemical oxidation of conducting polymers," Synthetic Metals, vol. 76, pp. 293-295, 1996.
15. M. Shahinpoor, K. J. Kim, "Effects of counter-ions on the performance of IPMCs," in Proc. SPIE Smart Structures and Materials: Electroactive Polymer Actuators and Devices, vol. 3987, pp. 110-120, Newport, CA, March 2000.
16. G. M. Spinks, L. Liu, G. G. Wallace, D. Zhou, "Strain response from polypyrrole actuators under load," Advance Functional Materials, vol. 12, no. 6-7, pp. 437-440, 2002.
17. J. M. Gere, Mechanics of Materials, Nelson Thornes, Cheltenham, England, 2002.